Energy, Mines and Resources Canada | Énergie, Mines et Ressources Canada

CANMET

Canada Centre for Mineral and Energy Technology | Centre canadien de la technologie des minéraux et de l'énergie

AN EVALUATION OF WELD METAL TOUGHNESS FOR LOW TEMPERATURE OFFSHORE STRUCTURE APPLICATIONS

J.A. Gianetto and J.E.M. Braid
Welding Section

December 1985

27pp

PHYSICAL METALLURGY RESEARCH LABORATORIES
DIVISION REPORT PMRL 85-71(TR)

MICROMEDIA

PHYSICAL METALLURGY RESEARCH LABORATORIES
REPORT PMRL 85-71(TR)

AN EVALUATION OF WELD METAL TOUGHNESS FOR LOW TEMPERATURE OFFSHORE STRUCTURE APPLICATIONS

by

J.A. Gianetto and J.E.M. Braid

ABSTRACT

Two welds were prepared in 25 mm thick C-Mn microalloyed steel plate using the shielded-metal-arc (SMA) and submerged-arc (SA) welding processes. The toughness properties of the two welds were evaluated using the Charpy and Crack Tip Opening Displacement (CTOD) tests. The Charpy notch toughness of the SMA weld was slightly higher than the SA weld. The CTOD properties of the SA weld were superior to those of the SMA weld in tests conducted at -10° and -30°C. The fractures in both welds were found to initiate from large (>1 μm) non-metallic inclusions and the differences have been explained using a model which considers notch tip acuity and the size distribution of inclusions. It is recommended that both a blunt notch-impact test (Charpy) and a sharp crack test (CTOD) be used to properly evaluate the toughness properties of welded joints.

LABORATOIRES DE RECHERCHE EN MÉTALLURGIE PHYSIQUE
RAPPORT: PMRL 85-71(TR)

UNE ÉVALUATION DE LA TENACITÉ DU MÉTAL SOUDÉ POUR APPLICATIONS SUR LES STRUCTURES HORS DES CÔTES À BASSE TEMPÉRATURE

PAR

J.A. GIANETTO et J.E.M. BRAID

RESUME

Deux soudures fûrent réalisées sur des plaques d'acier micro-allié au C-Mn en utilisant les procédés de soudage avec électrode enrobée (SMA) et à arc submergé (SA). Les propriétés de résilience des deux soudures fûrent évaluées par les tests Charpy et d'écartement de la base de la fissure (CTOD). La résilience des entailles Charpy de la soudure SMA était sensiblement plus élevée que celle de la soudure SA. Les propriétés CTOD de la soudure SA était supérieures à celles de la soudure SMA dans les test exécutés à -10°C et -30°C. Les fractures dans les deux soudures fûrent initiées à partir de larges inclusions non-métalliques (>1μm) et les différences ont été expliquées en utilisant un modèle considérant l'acuité de la base des entailles et la distribution de la taille des inclusions. Il est recommandé d'utiliser à la fois, le test d'impact Charpy et le test CTOD pour évaluer les propriétés de résilience des joints soudés.

INTRODUCTION

The discovery of offshore oil and gas in such regions as Sable Island, Hibernia, North Labrador and the Beaufort Sea over the past decade has significantly increased the need to develop Canadian technology in order to recover these resources. Much of the technology available for the fabrication of drilling ships, production platforms and supply vessels has been developed for regions with less demanding environments, particularly the Gulf of Mexico and the North Sea.

The environmental conditions of Hibernia and the North Labrador regions are more severe with lower design temperatures (-17 to -20°C), sea ice and the presence of icebergs. The conditions in the Beaufort Sea and Arctic are also severe. Temperatures as low as -50°C and pack ice represent the main design obstacles. Because of the usually harsh conditions technology must be developed to provide the utmost in structural integrity. An integral part of all fabrication will be the joining of steels by welding. The weld metal requirements at temperatures much lower than previously required will necessitate the development of such technology.

Presently there is considerable research literature available concerning weld metal toughness (1,2), however, fracture toughness studies are limited for conditions likely to be experienced in Canadian offshore regions, i.e., testing at temperatures below -10°C. This paper deals with the preliminary study of the relationship between weld metal microstructures and the fracture toughness of C-Mn welds deposited by the shielded-metal-arc (SMA) and submerged-arc (SA) welding processes for use in offshore fabrication.

EXPERIMENTAL

MATERIAL SELECTION AND WELDING PROCEDURES

A C-Mn-V-Nb steel, 25 mm thick, similar to Lloyd's Registry LT60 and supplied by Algoma Steel Corp. was chosen for the initial development work required to establish welding procedures for both SMA and SA welding processes. The composition of this plate is shown in Table 1.

Commercially available consumables were selected for each process and their compositions are listed in Table 2. The shielded-metal-arc (OS2) welding procedure was developed for the vertical-up (3G) position, utilizing 3.2 mm diam electrodes of AWS E7018-1 classification. The welding parameters

used are given in Table 3. The wire-flux combination used for the SA weld (OS1) consisted of a 4.0 mm diam SD-3 wire and OP121TT basic agglomerated flux. Details of the welding parameters are shown in Table 4. The test plates were prepared to provide a single-V bevel and a double-V bevel joint design for the SMA and SA processes respectively. Backgouging was employed in both procedures to remove the root pass, before welding was completed on the final side. No preheat was used in either procedure, however, a maximum interpass temperature of 150°C was maintained throughout all welding. The joint designs, pass sequences and typical macrosections are shown in Fig. 1 and 2. The welds were inspected by radiography to ensure that the weld metal was sound.

MECHANICAL TESTING

The tensile properties of each weld were measured by testing longitudinal all-weld-metal tensile specimens. Charpy V-notch specimens were machined from each weldment transverse to the weld length and notched through-thickness at the centerline. These specimens were located in the region believed to exhibit the lowest toughness, namely the large as-deposited back pass of weld OS1 and the root region of weld OS2. Testing was performed in accordance with ISO standard R148-1960. The tests were carried out over the temperature range -60°C to +20°C to produce transition curves. The per cent shear and lateral expansion were also measured for each specimen. The weld metal fracture toughness was determined by crack-tip-opening-displacement (CTOD) tests (3) on full thickness, B x 2B, specimens. All specimens were notched through-thickness at the weld centerline. Each CTOD specimen was locally compressed to 1% total strain prior to fatigue cracking to relieve local residual stresses. Fatigue cracking was completed using an Amsler Vibrophore of 100 kN capacity to a target crack length between 0.45 W and 0.55 W. A total of nine CTOD specimens were tested at -30°C and -10°C. A displacement rate of 0.01 mm/s was used during the test. After testing, selected specimens were heat tinted at 150°C prior to being broken apart to facilitate measurements of stretch zones and ductile tearing. All specimens were examined to determine the fatigue crack lengths and for preparation of metallographic and fractographic samples.

METALLOGRAPHY AND FRACTOGRAPHY

Transverse sections from each weld were prepared for optical microscopy using standard metallographic techniques. The samples were etched in 2% nital to reveal the gross microstructural constituents of the as-deposited and reheated regions. Quantitative analysis were performed on the last as-deposited weld bead according to the Abson and Dolby scheme (4). A total of 1000 points were evaluated over a 50 x 20 grid system at the center of the weld bead.

Full thickness macrosections were prepared and etched in 2% nital to facilitate measurements of the percentage of as-deposited and reheated weld metals. The columnar (as-deposited), coarse-grained and fine-grained reheated proportions were quantified.

The inclusion volume fraction and size distribution were analyzed using a Cambridge Instruments Quantimet 900 on polished and unetched samples from each weld.

Fracture surfaces from selected CTOD specimens were examined in a scanning electron microscope (SEM) to identify the origin and mode of fracture.

RESULTS

WELD METAL COMPOSITION

The chemical composition for each weld deposit is shown in Table 2 along with those of the respective welding electrode wires. The compositions of the welds are attributed to dilution with the base material and element transfer from the electrodes and flux for the two processes. C, Mn, Si and S are influenced by both factors while the remaining elements are primarily a result of dilution from the base material. Copper in the SA weld (OS1) originates from both the base metal and the wire coating.

MECHANICAL PROPERTIES

The tensile properties of each weld, shown in Table 5, met the required levels of strength, elongation and reduction in area in accordance with the CSA W48 standards governing classification of the consumables used. The minimum yield strength for both specifications is 410 MPa which exceeds the nominal yield strength of the base plate (350 MPa).

The test results for the Charpy impact tests are shown in Table 6 and Fig. 3. The SMA weld (OS2) has a slightly lower transition temperature behaviour than the SA weld (OS1). The data trends (including % shear) also indicate that at 20°C, the SMA weld has reached its upper shelf level while the SA weld has not.

CTOD fracture toughness values from testing at -30°C and -10°C are shown in Table 7. In general the CTOD values are significantly higher for the SA weld (OS1) compared to the SMA weld (OS2) over the temperature range investigated. Following the calculation of required CTOD in as-welded construction by Pisarski and Harrison (5), a minimum value of 0.1 mm CTOD is required for 25 mm thick weldments. At -10°C this value is easily met by the SA weld while the SMA weld gives marginal values. For the SA weld tested at -30°, the required CTOD value was exceeded in 3 out of 5 tests while the SMA weld did not meet the requirements displaying brittle behaviour in 4 out of 5 tests.

WELD METAL MICROSTRUCTURE

The proportions of as-deposited and reheated weld metal, shown in Fig. 4, varied significantly between the welds. The SA weld (OS1) consisted of approximately 85% as-deposited weld metal compared with 46% for the SMA weld (OS2). This difference reflects both the lower heat input and increased number of passes required to fill the joint of the SMA weld compared to the SA weld.

The as-deposited, columnar structure of the SA weld (OS1), shown in Fig. 5, consisted of an acicular ferrite matrix delineated by grain boundary ferrite veins. The elongated grains represent the prior austenite grain structure which was subsequently transformed. The as-deposited structure of the SMA weld (OS2) is shown in Fig. 6 and consisted primarily of an acicular ferrite matrix delineated by a grain boundary ferrite component and areas of ferrite with second phase. The prior austenite grains in the SMA weld are not as elongated as those in the SA weld owing to the inclined columnar growth of vertical welds (6). Table 8 presents the results from point counting used to determine the microstructural constituents of the as-deposited material. The amounts of acicular ferrite (AF) are approximately the same for both welds. Small amounts (1-3%) of polygonal ferrite (PF) were also present in both welds. The main differences between the two welds as seen in Fig 5(b) and 6 (b) is the larger amount of ferrite with second phase (AC) (17%) in the SMA

weld compared with 2% in the SA weld. The total percentage of boundary ferrite (GF and AC) was close for both welds.

The coarse-grain reheated weld metal, shown in Fig. 7, consisted of equiaxed prior austenite grains containing an acicular ferrite matrix delineated by grain boundary ferrite. Areas of ferrite with second phase were also present. The fine grain reheated structures for both welds, shown in Fig. 8, consisted of polygonal ferrite and a carbide aggregate (pearlite). The SA weld had slightly more pearlite due to the higher carbon content and slower cooling rate. In general, the microstructural constituents of the SA weld were coarser than the SMA weld.

The volume fraction and size distribution of non-metallic inclusions for both welds is given in Table 9. Also shown is the amount of oxygen plus sulphur (O + S) determined by chemical analysis. The O + S levels correlate well with the measured volume fraction of inclusions for the two welds. The mean size of inclusions for both welds was approximately the same (0.9 μm), however, there were significantly more inclusions in the SMA weld (OS2) compared to the SA weld (OS1). Also, the SMA weld had a greater number of large (>1 μm) inclusions.

DISCUSSION

The toughness of weld metals is controlled by two basic factors; microstructure and strain (2). For both the SA and SMA welds the plate sizes and levels of restraint were the same. The amounts of carbon and nitrogen in the welds, shown in Table 2, were also approximately the same. Hence, the differences in measured toughness were not attributed to strain effects such as residual stresses and dynamic strain aging (7-9) and were thought to be primarily microstructure controlled.

The toughness of the two C-Mn welds showed a small difference in the lower shelf and transition region Charpy properties (Fig. 3) and a major difference in the CTOD results (Table 7). The trends in increasing energy with higher test temperatures and the % shear measured on the Charpy fracture surfaces given in Table 6 indicate that the SA weld (OS1) has not reached its upper shelf at +20°C while the SMA weld (OS2) is close to the upper shelf. The higher upper shelf energy for OS1 would be consistent with the observed lower oxygen and sulphur levels for this weld.

Microstructural examination of the two welds revealed no significant difference in the amount of acicular ferrite (66% for OS1 and 63% for OS2) in the as-deposited regions. The effectiveness of acicular ferrite as a barrier to continued crack propagation from regions of grain boundary ferrite and ferrite with second phase has been shown by Tweed and Knott (10). Cross-sections of fracture surfaces from both welds revealed the preference of cracks to propagate along grain boundary ferrite veins, particularly at fracture initiation sites in regions of high constraint, in agreement with references 9 and 10.

One of the main differences between the two welds was in the amount of as-deposited weld metal. Eighty-five per cent of the SA weld (OS1) was as-deposited compared to 46% for the SMA weld (OS2). In the vicinity where the Charpy specimens were removed (shown in Fig. 4) this becomes approximately 88% for OS1 and 35% for OS2. This may partially explain the slightly lower Charpy toughness values of the SA weld (OS1); the higher proportion of reheated weld metal in OS2 resulting in improved toughness (6,9-14). However, the trends are opposite for the CTOD results where a large difference in fracture toughness was measured.

Tweed and Knott (10) postulated from fractographic examination that weld metal inclusions larger than 1 μm diam can act as sites for cleavage crack initiation. Plastic deformation in coarse-grain boundary proeutectoid ferrite produced dislocation pileups and high stresses at inclusions. At a critical stress the inclusions cracked and brittle fracture could initiate from the broken inclusions. Later, McRobie and Knott (9) showed that such a mechanism also caused cleavage fracture initiation in reheated weld metal in polygonal ferrite grains. Fractographic examination of the welds in the present study confirms this type of mechanism as an important source of cleavage initiation as shown in Fig. 9. The size distribution of inclusions shown in Table 9 indicates that the SMA weld (OS2) has both a greater volume fraction and a larger number of inclusions $\geq$1 μm diam relative to the SA weld (OS1). The greater number of large inclusions increases the probability of such an inclusion existing in a vein of grain boundary ferrite. Thus, although the SA weld has a larger proportion of as-deposited weld metal the larger number of non-metallic inclusions acting as cleavage crack initiation sites results in lower toughness, as measured by CTOD, of the SMA weld.

The differences in toughness measured by both Charpy and CTOD tests can be qualitatively rationalized using the model of Ritchie et al. (15).

Considering inclusions of size >1 μm as cleavage initiation sites, the greater number of these inclusions in the SMA weld results in a smaller distance, ℓ, from the crack tip to an inclusion where the critical fracture event can occur compared to the SA weld in CTOD tests as shown in Fig. 10. The critical fracture event occurs when the stress in front of the crack tip, σ_{yy}, becomes greater than the fracture stress, σ_F, over the distance ℓ. For a rounded notch, as in a Charpy specimen, fracture occurs when the maximum value of σ_{yy} exceeds σ_F at the plastic-elastic interface (which is much greater than ℓ). In the case of the SA weld the measured notch toughness is slightly lower. This may be a result of a slightly lower average-fracture stress, σ_F, as a result of the larger amount of as-deposited material in this weld.

The differences in toughness measured by the two methods (Charpy vs. CTOD) highlights the problems faced when evaluating the performance of welded joints. Dawes (16) showed that it is not always possible to differentiate the toughness between welds using Charpy or sub-sized CTOD tests and it was necessary to test full thickness specimens to clearly determine the fracture behaviour of a given weld. Sub-size specimens do not properly sample the full range of microstructures, inclusion distributions and strain affected regions [i.e., sub-surface and root region Charpy properties in thick welds often have different notch toughness because of dynamic strain aging in the root region (7-9)]. Also, sub-size specimens do not reflect the higher constraint levels present in full thickness tests particularly for thick specimens. However, Charpy tests do give important information on dynamic effects and effects of blunt notches compared to the sharp cracks of CTOD specimens.

The results in this study and others (17,18) show that it is unlikely that Charpy and CTOD test results are inter-related. Dolby (19), however, has found useful empirical correlations between Charpy and full thickness CTOD providing the Charpy specimens are removed from the root region and the micromechanism of failure is the same as for the CTOD specimen.

CONCLUSIONS

1. Charpy test results gave an opposite ranking of toughness for the two welds compared to the CTOD test results. The differences have been explained using the model of Ritchie et al. which considers the difference between the sharp crack of the CTOD testpiece and the blunt notch of the Charpy testpiece.
2. The Charpy energy for the SMA weld was slightly higher than for the SA weld. At -10°C the SA weld easily met a 0.1 mm CTOD requirement while the SMA weld gave marginal results. At -30°C the SA weld gave marginal CTOD results while the SMA weld did not meet the 0.1 mm requirement.
3. The micromechanism of fracture in both welds was attributed to the initiation of cleavage cracks at non-metallic inclusions ≥ 1 μm in size.
4. The number and distribution of large size (>1 μm) non-metallic inclusions ahead of the crack tip is a major factor determining the fracture toughness of the weld metals tested. The SMA weld had a greater number of large size inclusions compared to the SA weld and a correspondingly lower fracture toughness.
5. The amount of as-deposited and reheated microstructures may be responsible for the small differences in Charpy notch toughness of the two welds. The larger proportion of reheated weld metal in the SMA weld giving improved notch toughness compared to the lower toughness of the SA weld which had a high proportion of as-deposited weld metal.
6. Both Charpy and full thickness CTOD tests should be used when evaluating the toughness of welded joints.

ACKNOWLEDGEMENTS

The authors would like to thank the following for their assistance during the course of this work: R.F. Orr for experimental welding, D.P. Lusk for radiographic inspection, Dr. B. Faucher and C. Trinque for CTOD testing, Dr. M. Shehata and B. Causault for inclusion characterization and Dr. J.T. McGrath for many useful discussions.

REFERENCES

1. Dolby, R.E. Metals Tech Vol. 10, 1983, pp 349-362.

2. Braid, J.E.M. and McGrath, J.T. Division Report ERP/PMRL 84-67(J); CANMET, Energy, Mines and Resources Canada; 1984.

3. British Standards Institution. Methods for crack opening displacement (COD) testing; BS5762: 1979; London; 1982.

4. Abson, D.J. and Dolby, R.E. IIW Doc. No. IX-J-29-80; 1980.

5. Pisarski, H.G. and Harrison, J.D. Proc. Int. Conf. Welding for Challenging Environments, Weld. Inst. of Canada; Toronto, Canada; October 1985.

6. Evans, G.M. Weld. Res. Abroad Vol. 29, No. 1, 1983, p 58.

7. Cochrane, R.C., Terry, P. and Garland, J.G. Weld. and Met. Fab. Vol. 44, No. 4 and 6, 1976, pp 316 and 439.

8. Berkhaut, C.F. and Van den Brink, S.H. Weld. and Met. Fab. Vol. 46, No. 5, 1978, p 347.

9. McRobie, D.E. and Knott, J.F. Met. Sci. and Tech. Vol. 1, 1985, p 357.

10. Tweed, J.H. and Knott, J.F. Met. Sci. Vol. 17, 1983, p 45.

11. Evans, G.M. Weld. Res. Abroad Vol. 29, No. 1, 1983, p 24.

12. Evans, G.M. Weld. Res. Abroad Vol. 29, No. 1, 1983, p 35.

13. Evans, G.M. Weld. Res. Abroad Vol. 29, No. 1, 1983, p 46.

14. Stout, R.D., McLaughlin, P.F. and Strunk, S.S. Weld. J. Vol. 48, 1969, p 155s.

15. Ritchie, R.O., Francis, B. and Server, W.L. Met. Trans. Vol. 7A, 1976, p 831.

16. Dawes, M.G. Weld. and Met. Fab. Vol. 40, 1972, p 95.

17. Kamath, M.S., Abson, D.J. and Garland, J.G. Weld. and Met. Fab. Vol. 46, No. 6, 1978, p 385.

18. Braid, J.E.M. and Gianetto, J.A. Division Report 85-44(OP-J); CANMET, Energy, Mines and Resources Canada; 1985.

19. Dolby, R.E. Weld. Inst. Report 109/1980; Weld. Institute; Abington, Cambridge; 1980.

Table 1 - Chemical composition of base material

Base Material	Elements %												
	C	Mn	Si	S	P	Al	Sn	Cu	Ni	Cr	Mo	V	Nb
LT60	0.12	1.3	.28	.011	.017	.025	.005	.155	.135	.150	.010	.050	.040

Table 2 - Composition of welding wires and deposits

Specimen	Elements %															
	C	Mn	Si	S	P	Al	Sn	Cu	Ni	Cr	Mo	V	Ti	Nb	O	N
Weld OS1	.08	1.48	.34	.007	.015	.015	.005	.150	.09	.09	.010	.020	.005	.020	.026	.0079
Wire SD-3	.10	1.65	.2	.014	.009	-	.02	.02	.03	.015	.010	.005	.005	.005	-	-
Weld OS2	.07	1.54	.4	.014	.014	.005	.002	.055	.035	.035	.010	.005	.005	.005	.044	.0060
Wire LA 18 Plus	.07	.45	.03	.016	.010	-	.02	.02	.03	.015	.010	.005	.005	.005	-	-

Table 3 - Welding parameters for SMA weld (OS2)

Side 1 Pass No.	Current DCRP (amps)	Voltage (volts)	Run Out Length (mm)	Travel Speed (mm/min)	Heat Input (kJ/mm)
1	120	22	76	68	2.3
2	135	22	71	66	2.7
3	135	22	76	71	2.5
4	135	22	102	102	1.8
5-10	135	22	76	76	2.3
Side 2 11-14	135	22	102	102	1.8

Table 4 - Welding parameters for submerged-arc weld (OS1)

Side 1 Pass No.	Current DCRP (amps)	Voltage (volts)	Wire Feed Speed (mm/min)	Travel Speed (mm/min)	Elect. Stick Out (mm)	Heat Input (kJ/mm)
1	600	32	1270	406	32	2.8
2	600	34	1270	406	32	3.0
Side 2						
3	600	32	1270	406	32	2.8
4-7	600	33	1270	406	32	2.9

Table 5 - Weld metal tensile properties

Weld	Yield Strength MPa	Ultimate Strength MPa	Elongation %	Reduction in Area %
OS1	523	634	28	66
	537	634	27	67
OS2	543	615	29	74
	541	606	23	70

Table 6 - Impact properties of weld deposits

	OS1 (SAW)			OS2 (SMAW)		
Temperature (°C)	Energy (Joules)	% Shear	Lateral Expansion mil	Energy (Joules)	% Shear	Lateral Expansion mil
	144	89	74	138	88	72
RT (20°C)	143	77	66	128	88	62
	146	81	80	-	-	-
(avg.)	(145)	(82)	(73)	(133)	(88)	(67)
	84	65	48	132	85	70
0°C	98	63	64	123	79	60
	128	77	70	117	76	58
(avg.)	(103)	(68)	(61)	(124)	(80)	(63)
	97	56	46	125	72	60
-10°C	96	56	58	118	72	60
	74	59	44	90	67	50
(avg.)	(89)	(57)	(49)	(111)	(70)	(57)
	67	44	36	76	52	38
-20°C	68	48	40	62	62	36
	67	56	34	67	59	48
(avg.)	(67)	(49)	(37)	(68)	(58)	(41)
	50	36	28	58	52	28
-40°C	48	44	24	54	40	38
	44	40	30	45	44	26
(avg.)	(47)	(40)	(27)	(52)	(45)	(31)
	30	36	20	58	42	32
-50°C	50	40	32	27	26	14
	41	36	24	54	33	26
(avg.)	(40)	(37)	(25)	(46)	(34)	(24)
	16	-	-	17	16	4
-60°C	20	27	12	26	21	10
	38	35	20	20	30	14
(avg.)	(25)	(31)	(16)	(21)	(22)	(9)

Table 7 - CTOD results

Weld	Temperature °C	CTOD (mm)
OS1	-10	0.93*
		1.03*
		0.22
		0.95*
	-30	0.09
		0.24
		0.05
		0.26
		0.13
OS2	-10	0.11
		0.11
		0.07
		0.08
	-30	0.04
		0.06
		0.03
		0.20
		0.04

All CTOD values are δ_c;
except * which were δ_m.

Table 8 - Microstructural constituents in as-deposited weld metals

	%			
Weld	AF	GF	PF	AC
OS1	66	29	3	2
OS2	63	19	1	17

AF = acicular ferrite

GF = grain boundary ferrite

PF = polygonal ferrite

AC = ferrite with second phase

Table 9 - Inclusion volume fraction and size distribution

	Volume	Mean	Size Distribution					O + S
Weld	Fraction	Size	0-1	1-2	2-3	3-4	4-5	%
OS1	0.30	.897 μm	9553	1374	10	3	0	.033
OS2	0.57	.909 μm	22956	3635	27	8	4	.058

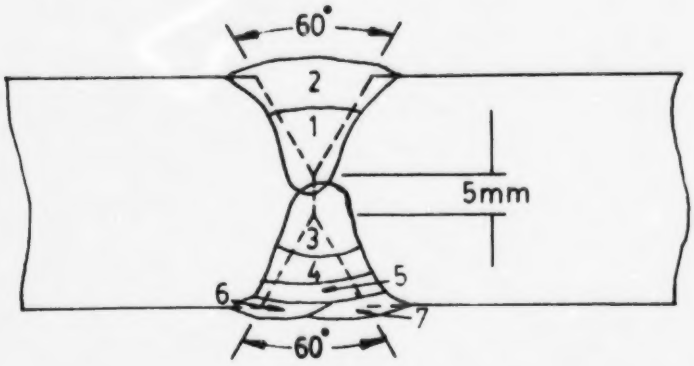

Fig. 1(a). Joint design and pass sequence for the submerged arc weld OS1. (neg 13383)

Fig. 1(b) Macrosection of completed joint. (neg 14026)

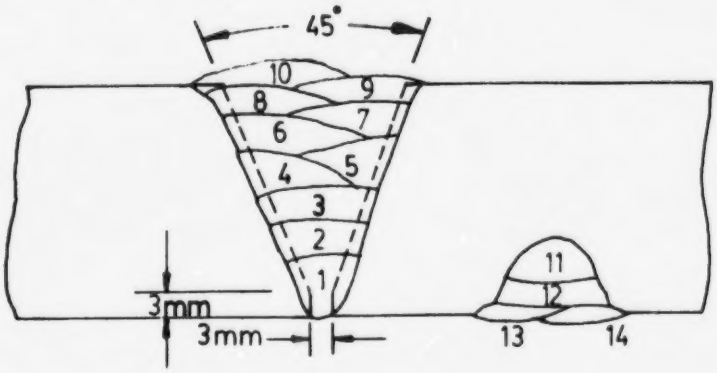

Fig. 2(a). Joint design and pass sequence for the shielded metal arc weld OS2. (neg 13382)

Fig. 2(b). Macrosection of completed joint. (neg 14027)

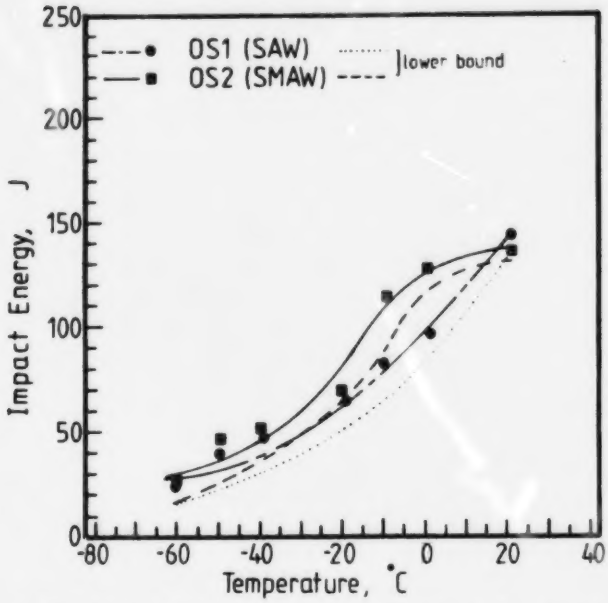

Fig. 3. Charpy impact transition curves for both weld metals. (neg 13381)

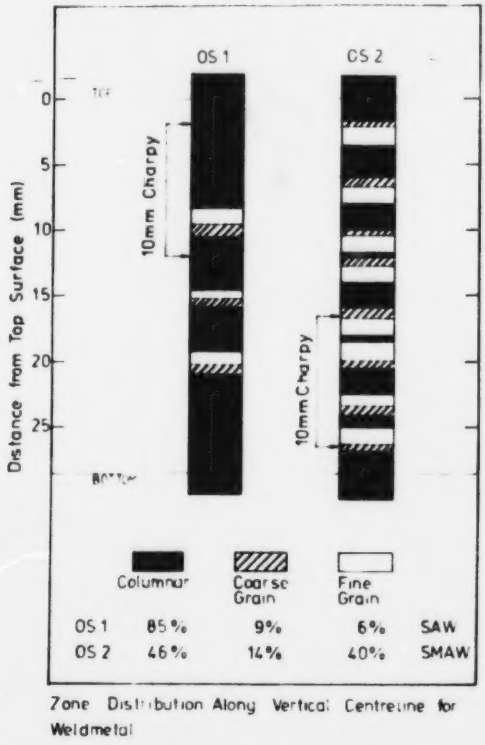

Fig. 4. Distribution of as-deposited and reheated weld microstructures along weld centre line for the SMA and SA welds. (neg 13384)

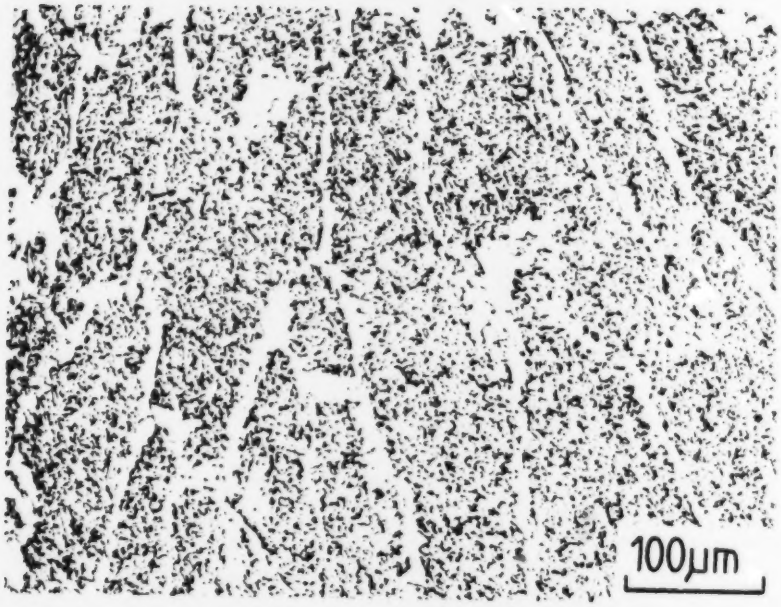

(a) (neg 14029)

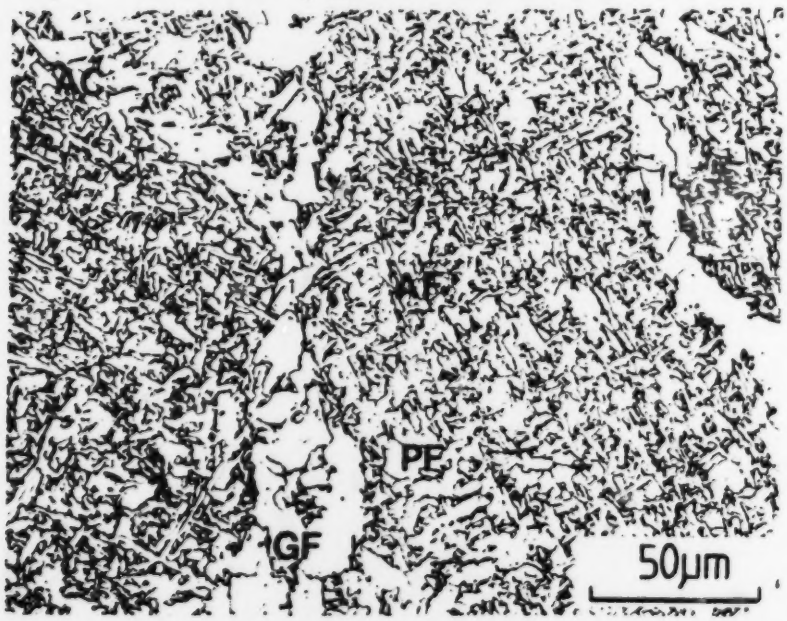

(b) (neg 14028)

Fig. 5. (a) As deposited columnar weld metal microstructure of SA weld OS1 (b) microstructural constituents; acicular ferrite (AF) grain boundary ferrite (GF) ferrite with aligned second phase (AC) and polygonal ferrite (PF).

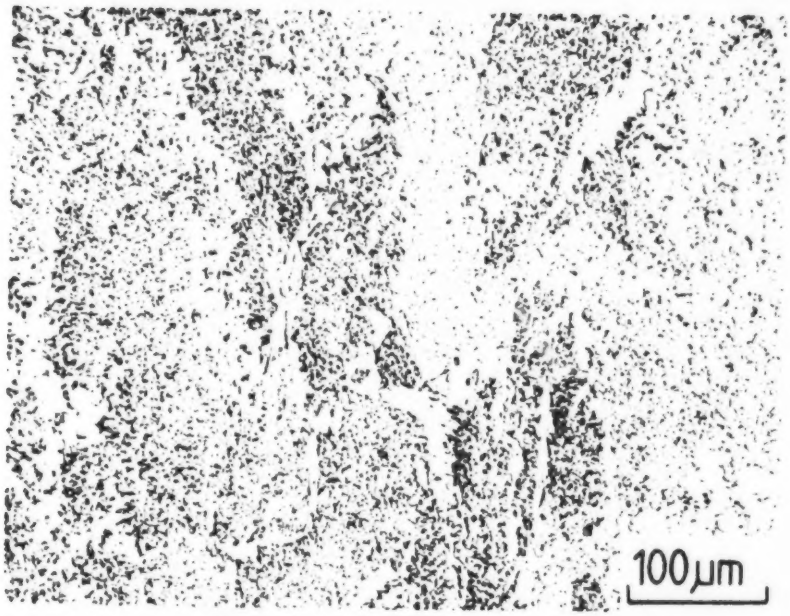

(a) (neg 14030)

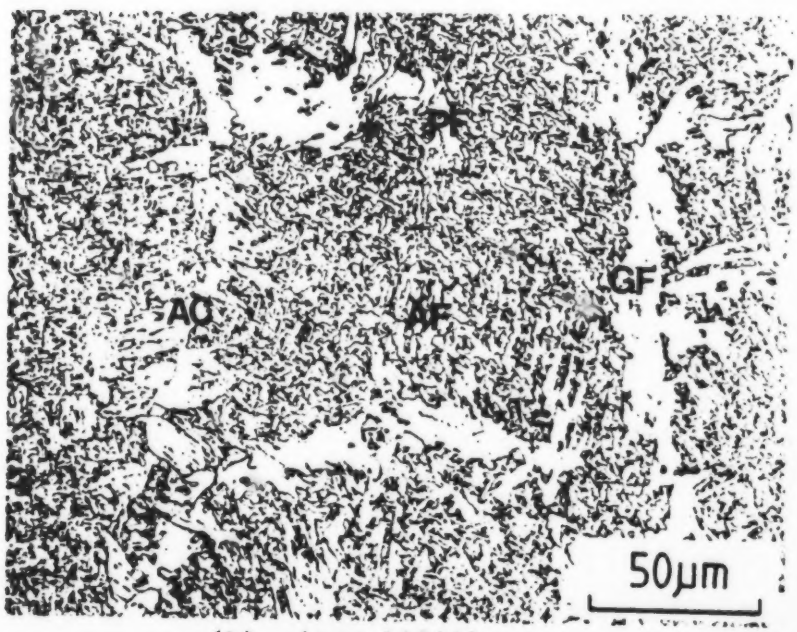

(b) (neg 14031)

Fig. 6. (a) As deposited columnar weld metal of SMA weld OS2, (b) Microstructural constituents.

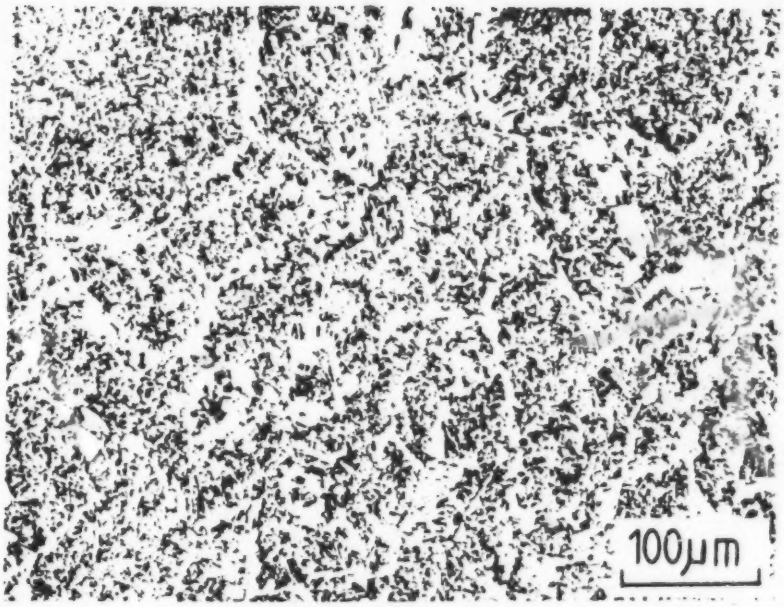

(a) (neg 13880)

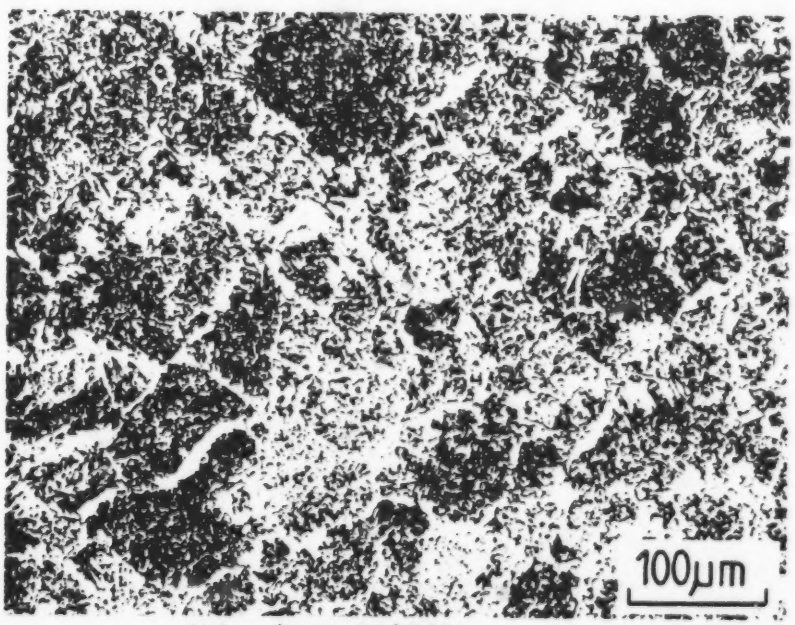

(b) (neg 13879)

Fig. 7. Coarse grain reheated weld metal microstructures (a) weld OS1; (b) weld OS2.

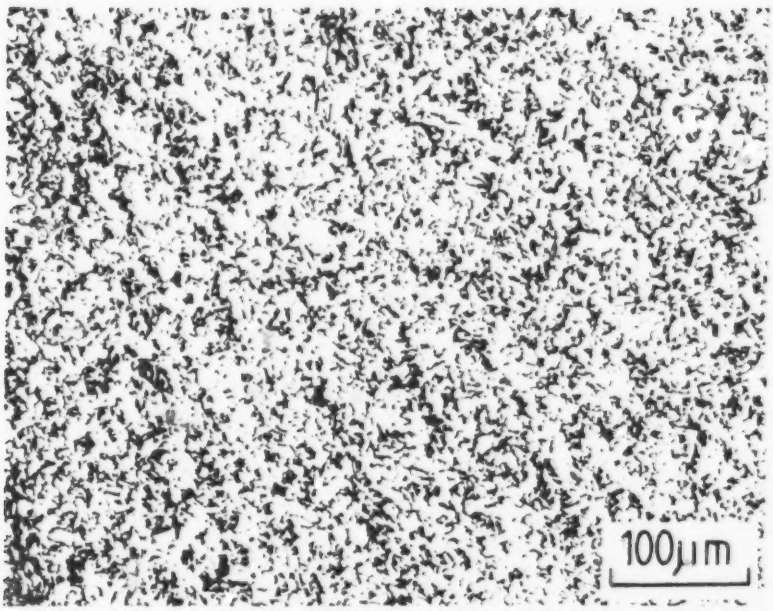

(a)

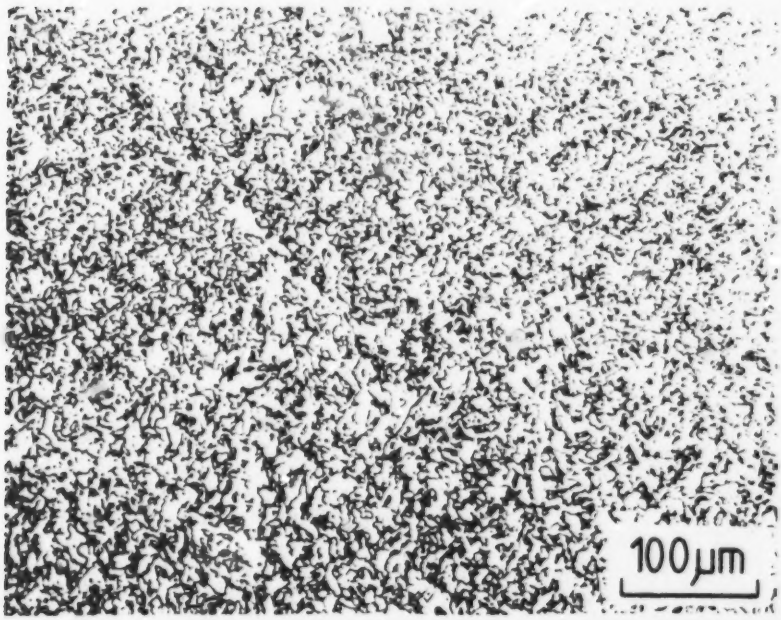

(b)

Fig. 8. Fine grain reheated weld metal microstructures. (a) weld OS1 (b) weld OS2. (neg 11358, 11359)

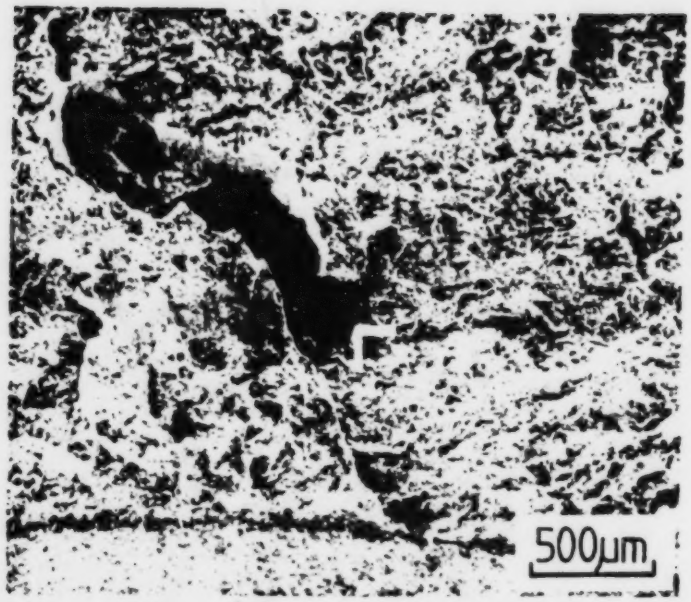

(a)

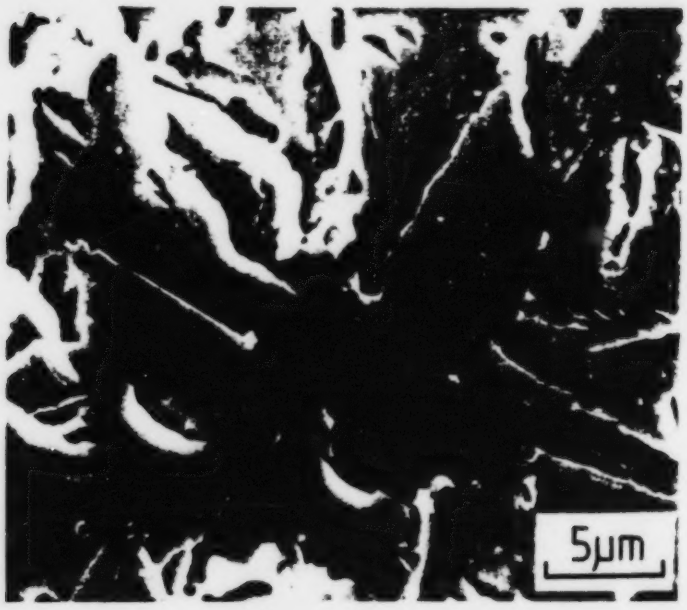

(b)

Fig. 9. Cleavage failure in CTOD testpiece tested at -30°C. Initiation, indicated in (a) occured at a non-metallic inclusion, (b) weld OS1.

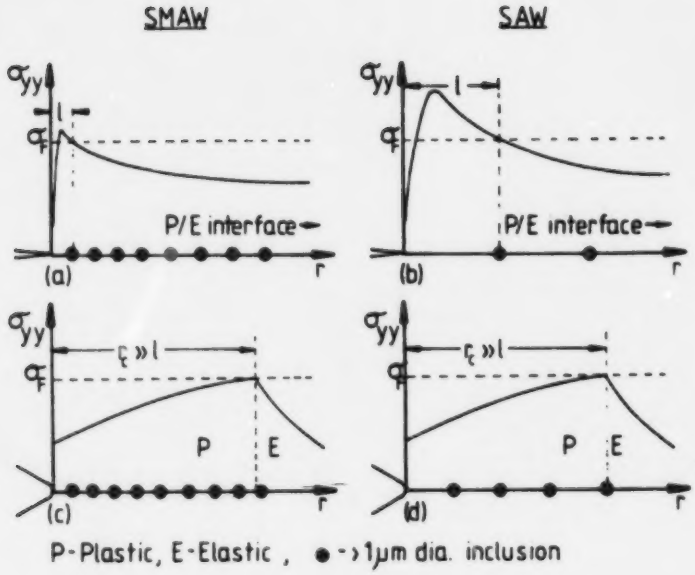

Fig. 10. Stress distribution as a function of distance, r, from sharp crack tip (a and b) and rounded notch (c and d). For sharp cracks, fracture occurs when the stress, σ_{yy}, exceeds the critical fracture stress, σ_F over the distance L. For rounded notches, fracture occurs when the stress, σ_{yy}, reaches σ_F. (neg 14032)